Peridotite, kimberlite, and carbonatite explained in the system $CaO-MgO-SiO_2-CO_2$

Peter J. Wyllie
Department of Geophysical Sciences
University of Chicago
Chicago, Illinois 60637

Wuu-Liang Huang
Department of Geology
National Taiwan University
Taipei, Taiwan

ABSTRACT

The key to the origin of carbonatite and kimberlite lies in the system $CaO-MgO-SiO_2-CO_2$. Increase in pressure causes a carbonation reaction in the peridotite assemblage as follows: forsterite + clinopyroxene + $CO_2 \rightleftharpoons$ orthopyroxene + carbonate (Ca:Mg::70:30). This reaction passes through 15 kb–960°C with slope 45 b/°C and terminates at an invariant point near 25 kb–1200°C, where melting begins. This intersection of the carbonation reaction with the solidus introduces primary carbonate minerals alongside peridotite minerals on the liquidus surface. At 20 kb the melting temperature of the peridotite assemblage Fo + Opx + Cpx is lowered 75°C by solution of about 5 wt percent CO_2. The liquid corresponds to undersilicated basic magma. Stabilization of carbonate increases CO_2 solubility in the liquid, and above 25 kb the liquidus reaction involving Fo + Opx + Cpx + CO_2 sweeps down through 400°C via a pressure maximum at 32 kb to meet the invariant point at 25 kb. The peridotite solidus curve at higher pressures involves fusion of silicates and carbonates, producing a carbonatitic liquid with more than 45 wt percent CO_2. Progressive fusion produces a kimberlitic liquid. There is an intricate series of reactions between 25 kb and 35 kb involving changes in silicate and carbonate phase fields on the CO_2-saturated liquidus surface. Fractional crystallization of CO_2-bearing undersilicated basic magmas at most pressures yields residual kimberlite and carbonatite. Kimberlite and carbonatite magmas rising from the asthenosphere evolve CO_2 as they reach a reaction boundary at a depth of about 100 to 80 km. This contributes to their explosive eruption. Free CO_2 cannot coexist with subsolidus mantle peridotite with normal temperature distributions. CO_2 appears to be as effective as H_2O in causing incipient melting in the asthenosphere.

INTRODUCTION

There is currently much interest in the effects of CO_2 and H_2O on magmatic processes in the mantle. Experiments with realistic bulk compositions, involving very small proportions of the volatile components, produce only trace amounts of liquid, which are difficult to study in detail. The relationships of the liquids with CO_2 to the mantle peridotite minerals—forsterite, orthopyroxene, and clinopyroxene—can be examined in detail in the carbonate-rich part of the system CaO-MgO-SiO_2-CO_2. The key to the petrogenetic links between carbonatite, kimberlite, and peridotite lies in the intersection of a decarbonation reaction with the solidus curve. Free CO_2 cannot normally exist in the mantle; it reacts with peridotite to produce a carbonate solid solution with composition about 7:3::Ca:Mg. Carbonatite and kimberlite are produced as primary magmas from carbonated mantle peridotite only at depths greater than 80 km and at moderate temperatures.

DECARBONATION REACTIONS

Bowen's (1940) petrogenetic grid was based initially on a series of decarbonation reactions in the system CaO-MgO-SiO_2-CO_2, with starting assemblages involving mixtures of calcite, dolomite, magnesite, and quartz, representing siliceous dolomites. The successive reactions introduce the silicate minerals enstatite, forsterite, diopside, and wollastonite, among several others, and addition of H_2O introduces tremolite. Extension of these reactions to mantle pressures and higher temperatures produces significant solid solution in the pyroxene and carbonate minerals. The minerals produced by the decarbonation reactions include forsterite, orthopyroxene, and clinopyroxene. These are commonly used to model mantle processes in the system CaO-MgO-SiO_2.

There are six decarbonation reactions at pressures above 10 kb that involve the mantle minerals. These are numbered in the direction of progressive decarbonation according to a scheme presented in detail elsewhere (Wyllie and Huang, in prep.).

Abbreviations for the minerals are explained in the legend to Figure 1, which illustrates reaction (6):

(1) $MC + Qz \rightleftharpoons En + CO_2$
(2) $Cm + Qz \rightleftharpoons Opx + Cd + CO_2$
(3) $MC + En \rightleftharpoons Fo + CO_2$
(4) $Cm + Opx \rightleftharpoons Fo + Cd + CO_2$
(5) $Cd + Opx + Qz \rightleftharpoons Cpx + CO_2$
(6) $Cd + Opx \rightleftharpoons Cpx + Fo + CO_2$

Maximum carbonation in the system is represented by the coexistence of quartz, carbonate, and CO_2 (Fig. 1). With each decarbonation reaction, produced either by temperature increase or by pressure decrease, the surface connecting quartz-carbonates is broken by the appearance of a stability field involving one or more of the silicate minerals that are behind this surface, farther away from the CO_2 apex of the tetrahedron. Figure 1 shows the compositions of pyroxenes Opx + Cpx and carbonates Cm + Cd coexisting across solvi for a temperature of 1150°C.

Reaction (1) breaks the join quartz-magnesite and replaces it with enstatite-CO_2, and reaction (2) is the equivalent quaternary reaction with solid solution in Opx and Cm, which introduces dolomite solid solution, Cd, across the carbonate solvus. Reaction (3) in the system MgO-SiO_2-CO_2, determined by Newton and Sharp (1975), replaces the join enstatite-magnesite with forsterite-CO_2, and reaction (4) is the equivalent quaternary reaction involving solid solutions Opx, Cm, and Cd. Reaction (5) uncovers the pyroxene solvus, exposing Cpx to CO_2, and reaction (6) brings all three mantle minerals, Fo, Opx, and Cpx, into coexistence with CO_2 and a carbonate, Cd, with composition between dolomite and calcite (Fig. 1). A similar reaction with a different carbonate was listed in an abstract by Eggler (1975). The reaction terminates at an invariant point near 25 kb, Q_6, where the assemblage is joined by a liquid (Fig. 2).

Newton and Sharp (1975) determined the position of reaction (3). We have confirmed this and also located the position of reaction (6) (Fig. 2). At 15 kb, reaction (3) occurs at 890°C, reaction (6) at 960°C, and both have a slope of 45 b/°C. Reaction (6) is thus situated within

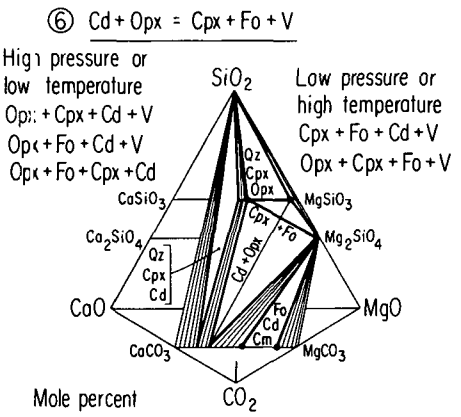

Figure 1. Isobaric isothermal diagram showing univariant decarbonation reaction (6), which involves mantle peridotite minerals olivine, orthopyroxene, and clinopyroxene. Phase fields shown are connected to CO_2. Abbreviations: Fo, forsterite; Opx, orthopyroxene; Cpx, clinopyroxene; Qz, quartz or other silica polymorphs; Cm, magnesite (MC) solid solution; Cd, dolomite solid solution. Compositions of coexisting Opx and Cpx and of coexisting Cm and Cd are based on solvus curves by Nehru and Wyllie (1974) and Irving and Wyllie (1975).

75°C and 3 kb of reaction (3), and reactions (4) and (5) occur within this narrow band on the *P-T* diagram.

CARBONATION OF MANTLE PERIDOTITE

Reaction (3) represents carbonation of forsterite in the system MgO-SiO_2-CO_2, which provides an upper pressure limit for the existence of free CO_2 in the mantle (Newton and Sharp, 1975). The peridotite carbonation reaction (6) illustrated in Figures 1 and 2 is situated about 3 kb lower than reaction (3). According to Ringwood's (1966) geotherms, Figure 2 confirms the conclusion of Newton and Sharp that free CO_2 cannot exist in the mantle except under conditions of unusually high temperature. Normally, CO_2 would be stored in the assemblage Fo + Opx + Cpx + Cd (see Fig. 1).

All of the reactions (1) through (6) are displaced to lower temperatures in the presence of CO_2-H_2O mixtures (see Kerrick, 1974, for a review). Therefore, if an aqueous pore fluid exists in the

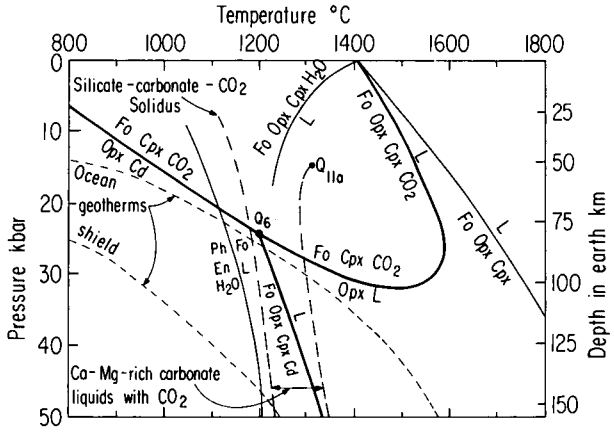

Figure 2. Univariant reactions for mantle peridotite assemblage Fo + Opx + Cpx with a small proportion of CO_2 compared with other reactions. Subsolidus reaction (6) extending to invariant point Q_6 is illustrated in Figure 1. Abbreviations as in legend for Figure 1, with addition: Ph, phlogopite.

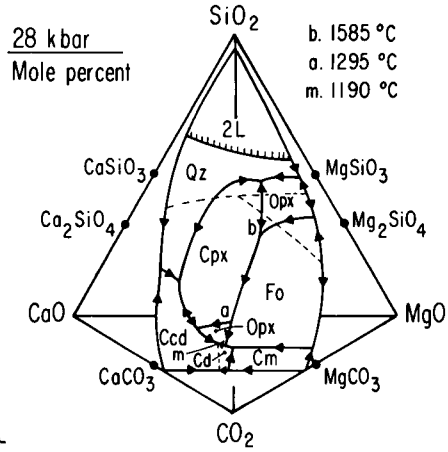

Figure 3. CO_2-saturated liquidus surface in CaO-MgO-SiO_2-CO_2 at 28 kb, partly schematic. Abbreviations as in Figure 1, with additions: Ccd, carbonate solid solution between calcite and dolomite; 2L, two immiscible liquids.

upper mantle, CO_2 could exist in the vapor phase along with partially carbonated peridotite. Addition of H_2O to mantle peridotite would stabilize amphibole and phlogopite. The fusion curve for phlogopite coexisting with mantle minerals (Modreski and Boettcher, 1973) is shown in Figure 2. The position of this reaction and the stability of amphibole are changed in the presence of H_2O-CO_2 vapors. Consideration of reactions such as these and the mineralogy of mantle samples might place limits on the possible ranges of CO_2/H_2O ratios in different depth intervals of the mantle.

CO_2-SATURATED LIQUIDUS-PHASE RELATIONSHIPS

Each of the decarbonation reactions terminates at an invariant point where it reaches melting temperatures, with as assemblage involving liquid, CO_2-vapor, carbonate minerals, and one of more of the silicate minerals Fo, Opx, Cpx, and Wo. The intersections of the decarbonation reactions with the solidus reactions in the system CaO-MgO-SiO_2-CO_2 produce an intricate series of liquidus reactions involving silicates and carbonates (Wyllie and Huang, in prep.). Figures 2 and 3 show some of these.

The melting relationships may be considered in two parts. Most investigators have been concerned with the high-temperature silicate-phase relationships in CaO-MgO-SiO_2—either volatile-free or with H_2O—and recently with CO_2. We have been studying the carbonate melting relationships (Irving and Wyllie, 1975; Huang and Wyllie, 1975) and the liquidus relationships between carbonates and silicates (Huang and Wyllie, 1974; Maaløe and Wyllie, 1975). These involve a series of reactions at considerably lower temperatures than those for the silicate-rich part of the system. The links between these two parts are provided by the subsolidus decarbonation reactions (see Yoder, 1973; Eggler, 1975).

Figure 2 compares the solidus for the volatile-free peridotite assemblage with the melting curve produced by the solution of CO_2. At 20 kb, the melting temperature is lowered through 75°C by the solution of about 5 wt percent CO_2 (Eggler, 1973, 1974). Our new data between 25 and 35 kb show the solidus in the presence of CO_2 sweeping down through 400°C via a pressure maximum at about 32 kb and terminating at the invariant point Q_6 near 25 kb and 1200°C. Increase in pressure not only stabilizes carbonate in the subsolidus mineral assemblage, but also in the liquid phase, and this produces a large increase in CO_2 solubility and the dramatic change in the reaction temperature. The solidus curve rising to higher pressures from Q_6 involves silicates and carbonates, without free CO_2.

The CO_2-saturated liquidus surface for 28 kb is illustrated in Figure 3. For compositions in the area SiO_2-$CaSiO_3$-$MgSiO_3$, the CO_2 solubility remains low, but for compositions ranging from the pyroxene join to the carbonate join, the CO_2 content of liquids increases progressively to more than 45 wt percent.

The dashed lines on the liquidus surface in Figure 3 show where the joins Wo-En-CO_2 and Fo-Di-CO_2 intersect it. At low pressures, the liquid *b* lies within the dashed triangle, but Eggler (1974) showed that somewhere between 15 and 30 kb it crosses the join Fo-Di, becoming larnite-normative. Eggler reported a value of 1565°C for *b* at 30 kb, and this is used to plot the position of the melting reaction in Figure 2. Huang and Wyllie (1974) reported a liquidus-field boundary between Fo and Cpx extending down from *b* toward the low-temperature carbonate-rich liquids represented in Figure 3 by the liquidus minimum, *m*, whose position is controlled by the liquidus minimum in the carbonate join (Irving and Wyllie, 1975). This minimum, and related reactions at other pressures, is represented in Figure 2 by the dashed-line solidus at a temperature slightly below Q_6. The temperature interval for the existence of carbonate-rich liquids with compositions in the general area

between *m* and *a* in Figure 3 is also indicated. The CO_2-free solidus reaction rising to higher pressures from Q_6 in Figure 2 would be represented in Figure 3 by a point behind the liquidus surface, somewhat further away from the CO_2 apex than liquids *m* and *a*, but with similar high content of dissolved carbonates.

Figure 2 shows that at 28 kb, the melting reaction for the assemblage Fo + Opx + Cpx + CO_2 is intersected twice, and the liquid compositions are represented in Figure 3 by the higher temperature liquid *b* and the lower temperature liquid *a* with much more dissolved CO_2. With increasing pressure, points *b* and *a* approach each other, becoming coincident at 32 kb (Fig. 2). At higher pressures, the CO_2-saturated liquidus fields for forsterite and clinopyroxene are separated by the field for orthopyroxene, and CO_2-saturated liquids cannot exist in equilibrium with the peridotite assemblage.

MAGMA GENERATION AND CRYSTALLIZATION

Partial fusion of the peridotite assemblage produces forsterite-normative liquids that represent basalt, with compositions in the forsterite to pyroxene range. At 20 kb, the melting temperature is lowered through more than 400°C by the solution of about 20 wt percent H_2O, as shown in Figure 2, and the liquid produced is quartz-normative (Kushiro, 1972). In contrast with CO_2 the liquid is depleted in SiO_2 (Fig. 3), becoming larnite-normative between 15 kb and 30 kb (Eggler, 1974). At 25 kb the solidus for peridotite with CO_2 drops abruptly from 1575°C to 1200°C (at Q_6), and at higher pressures the first liquid produced is carbonatitic, with less than 10 wt percent dissolved silicates in liquid with composition near dolomite. Within the limited pressure interval corresponding to the depths from 80 km to 100 km, there are remarkable changes in the compositions of liquids coexisting with peridotite mineral assemblages containing CO_2; there are two liquids occurring at different temperatures, one representing kimberlite (*b*) and the other carbonatite (*a*).

These results indicate that partial fusion of mantle peridotite with CO_2 at depths shallower than 80 km produces basaltic magmas, which become more undersaturated in silica with increasing depth. At depths greater than 80 km, the first magmas produced in trace quantities (at much lower temperatures) are carbonatites. With progressive fusion, these are converted to kimberlite and eventually, at considerably higher temperatures, to basaltic magmas.

Crystallization of the high-temperature undersilicated basic magmas with dissolved CO_2 yields residual kimberlite and carbonatite magmas. If these magmas fractionate without maintaining equilibrium with the host mantle peridotite, the residual liquids can reach the liquidus surface in Figure 3 and evolve CO_2. The final carbonatite reach the dashed-line solidus in Figure 2, corresponding to the liquidus minimum *m* in Figure 3.

Carbonatite and kimberlite generated from mantle periodotite at depths greater than 100 km are undersaturated with CO_2. Figure 2 shows that these magmas rising from the asthenosphere must evolve CO_2 at a depth of 100 to 80 km, which corresponds approximately to the lithosphere-asthenosphere boundary. This would certainly contribute to their explosive eruption. The undersilicated basic magmas generated at higher temperatures do not have the same tendency to evolve CO_2, except as a consequence of uprise to much shallower levels or of advanced crystallization.

In the presence of CO_2 and H_2O, the phase relationships become more complex, and the possible processes of fusion and crystallization become more varied.

SEISMIC LOW-VELOCITY ZONE

One explanation for the seismic low-velocity zone is that traces of H_2O in mantle peridotite cause incipient melting through the asthenosphere (Lambert and Wyllie, 1968). Green (1972) argued that the presence of CO_2 bubbles in peridotite xenoliths transported from the asthenosphere in kimberlites or alkalic basalts indicated that the asthenosphere was dry and not partially melted.

Figure 2 shows that free CO_2 cannot coexist in equilibrium with subsolidus mantle peridotite with normal temperature distributions. Apparently, the origin of CO_2 bubbles in mantle xenoliths must be associated with relatively low temperature diapiric uprise or with relatively high temperature magmatic processes. In the depth range of the asthenosphere, CO_2 appears to be as effective as H_2O in causing incipient melting in mantle peridotite.

REFERENCES CITED

Bowen, N. L., 1940, Progressive metamorphism of siliceous limestone and dolomite: Jour. Geology, v. 48, p. 225–274.

Eggler, D. H., 1973, Role of CO_2 in melting processes in the mantle: Carnegie Inst. Washington Year Book 72, p. 457–467.

— 1974, Effect of CO_2 on the melting of peridotite: Carnegie Inst. Washington Year Book 73, p. 215–224.

— 1975, Carbonate generation by a reaction relation in the system CaO-MgO-SiO_2-CO_2 at 30 kbar pressure: EOS (Am. Geophys. Union Trans.), v. 56, p. 470.

Green, H. W., 1972, A CO_2-charged asthenosphere: Nature, v. 238, p. 2–5.

Huang, W. L., and Wyllie, P. J., 1974, Eutectic between wollastonite II and calcite contrasted with thermal barrier in MgO-SiO_2-CO_2 at 30 kilobars, with applications to kimberlite-carbonatite petrogenesis: Earth and Planetary Sci. Letters, v. 24, p. 305–310.

— 1975, Melting relationships in the systems CaO-CO_2 and MgO-CO_2 to 33 kilobars: Geochim. et Cosmochim. Acta (in press).

Irving, A. J., and Wyllie, P. J., 1975, Subsolidus and melting relationships for calcite, magnesite and the join $CaCO_3$-$MgCO_3$ to 36 kb: Geochim. et Cosmochim. Acta, v. 39, p. 35–53.

Kerrick, D. M., 1974, Review of metamorphic mixed-volatile (H_2O-CO_2) equilibria: Am. Mineralogist, v. 59, p. 729–762.

Kushiro, I., 1972, Effect of water on the composition of magmas formed at high pressures: Jour. Petrology, v. 13, p. 311–334.

Lambert, I. B., and Wyllie, P. J., 1968, Stability of hornblende and a model for the low velocity zone: Nature, v. 219, p. 1240–1231.

Mariøe, S., and Wyllie, P. J., 1975, The join grossularite-calcite through the system CaO-Al_2O_3-SiO_2-CO_2 at 30 kilobars: Crystallization range of silicates and carbonates on the liquidus: Earth and Planetary Sci. Letters (in press).

Modreski, P. J., and Boettcher, A. L., 1973, Phase relationships of phlogopite in the system K_2O-MgO-CaO-Al_2O_3-SiO_2-H_2O to 35 kilobars: A better model for micas in the interior of the earth: Am. Jour. Sci., v. 273, p. 385–414.

Nehru, C. E., and Wyllie, P. J., 1974, Electron microprobe measurement of pyroxenes coexisting with H_2O-undersaturated liquid in the join $CaMgSi_2O_6$-$Mg_2Si_2O_6$-H_2O at 30 kilobars, with applications to geothermometry: Contr. Mineralogy and Petrology, v. 48, p. 221–228.

Newton, R. C., and Sharp, W. E., 1975, Stability of forsterite + CO_2 and its bearing on the role of CO_2 in the mantle: Earth and Planetary Sci. Letters (in press).

Ringwood, A. E., 1966, Mineralogy of the mantle, *in* Hurley, P. M., ed., Advances in Earth science: Cambridge, Mass., M.I.T. Press, p. 357–399.

Yoder, H. S., Jr., 1973, Akermanite-CO_2: Relationship of melitite-bearing rocks to kimberlite: Carnegie Inst. Washington Year Book 72, p. 449–457.

ACKNOWLEDGMENTS

Reviewed by A. T. Anderson and J. R. Goldsmith.

Supported by National Science Foundation Grant GA-41730, and by the Materials Research Laboratory of the National Science Foundation.

MANUSCRIPT RECEIVED JULY 3, 1975

MANUSCRIPT ACCEPTED AUG. 12, 1975